50th AIAA/ASME/ASCE/AHS/ASC Structures, Structural Dynamics, and Materials Conference
17th
4 - 7 May 2009, Palm Springs, California

AIAA 2009-2571

A Fast Tool for Structural Sizing, Aeroelastic Analysis and Optimization in Aircraft Conceptual Design

L. Cavagna*†, S. Ricci‡, L. Riccobene§

Dipartimento di Ingegneria Aerospaziale, Politecnico di Milano, Milano, 20156*, Italy*

Most of procedures available in conceptual design estimate airframe weight by statistical methods and do not take into account for aeroelastic requirements, postponing them to successive more detailed design phases. If the former task is not based on sound structural principles, the estimation will be likely to be unreasonable and results in serious difficulties, especially when non-conventional layouts are considered. Indeed, a large error in weight estimation will usually have far-reaching effects in the whole project; such errors have sometimes been the main factors in the unsuccessful designs. Furthermore, the late discovery of adverse aeroelastic issues may result in significant re-design costs, considerable changes in the structural design, limitations in flight envelope, weight penalties, and in some cases, it may even require to actually close the project. Thus, in order to overcome the insurgence of these issues, the influence of deformability on flight and handling performances, on structural weight and on design costs needs to be taken into account as early as possible in the design process.
NeoCASS (Next generation Conceptual Aero-Structural Sizing Suite) enables the creation of efficient low-order, medium fidelity models particularly suitable for structural sizing, aeroelastic analysis and optimization at the conceptual design level. It provides the total structural weight on physical basis, reducing to the minimum the adoption of statistics, and includes aeroelastic requirements and performances from the very beginning of the conceptual design phase. The whole methodology is based upon the integration of geometry construction, aerodynamic and structural analysis codes that combine depictive, computational, analytical, and semiempirical methods, validated in an aircraft design environment.

I. Introduction

The estimation of the structural weight is an important part of the conceptual design of an airplane. Obviously, it is impossible to wait until the airplane is completely designed, yet, it is necessary to know, with considerably accuracy, how much the airplane will weigh and what is the stiffness distribution to preclude failures and to satisfy strength, stiffness and, more generally speaking, aeroelastic constraints. The structural design of an airframe is indeed determined by multidisciplinary criteria such as stress, fatigue, buckling, flutter, control surface effectiveness, manufacturing and costs to mention a few.

Being most of the life-cycle cost of an aircraft incurred during the conceptual design phase, the earlier an appropriate conceptual configuration can be found, the more economical the whole design process will be, avoiding costly later redesign and corrections. Analytical formulas for structural weight prediction can be adopted (see the books by Raymer[1] and Torenbeek[2]), usually relating the weight of existing aircraft to various parameters known to affect the structural weight, i.e. gross weight, span, maximum load factor. Weight formulas of this type have serious disadvantages since extrapolation of the curves considerably beyond the range of the basic data may be misleading. Radical changes in configuration such as innovative layouts, may also introduce serious errors; it appears as quite unreliable to adopt statistical-based approaches where no enough knowledge is available, as in case of unconventional configurations and new technologies such as Sensorcraft[3,4] and Blended Wing Body aircraft.[5] The use of statistical based approaches for the structural

*Ph.D. fellow, Dipartimento di Ingegneria Aerospaziale, Politecnico di Milano, Milano, 20156, Italy.
†Now at FOI, Swedish Defence Research Agency, 164 90 Stockholm, Sweden.
‡Associate Professor, M.Eng. Ph.D., Dipartimento di Ingegneria Aerospaziale, Milano, 20156, Italy. AIAA Member.
§M.Eng., Ph.D. candidate, Dipartimento di Ingegneria Aerospaziale, Politecnico di Milano, Milano, 20156, Italy.

weight estimation means that the aircraft structure is practically absent till the preliminary design phase. Due to this choice, it is almost impossible to take into consideration aeroelastic requirements that in fact appear later during the design loop. New transport aircraft are very flexible and aeroelastic effects must be taken into consideration right from the beginning of the design phase so to avoid very expensive redesign during preliminary design phase or resulting weight penalties needed to satisfy aeroelastic requirements not previously taken into account.

The capability of including stiffness and aeroelastic constraints starting from the conceptual design is particularly challenging and important. Fluid-structure simulations are not very established in conceptual phase and optimization is even a big step further. As a matter of fact, aeroelastic requirements are usually not considered by the stress engineers determining structural sizes. In most cases there are significant time-delays until the design determined by the stress-group is available to aeroelasticians. Shortfalls in the aeroelastic behavior then demand additional efforts in order to find feasible solutions which may be non-optimal and expensive. Being aeroelastic synthesis particularly troublesome to determine, remedies to negative impacts of aeroelasticity on the design can be recovered by optimization strategies to ensure for example flutter-free structures, excellent multipoint performace characteristics, satisfying different classes of constraints.

Due to program requirements, the development cycles shrink continuously, while the technical demands grow. These contradictory requirements cannot be fulfilled by traditional sequential engineering. Because of typical sizes and complexity, there is a clear need for advanced tools integrating and accelerating the design process. Recently, new software systems specifically tailored for aircraft conceptual design have been proposed by Antoine et al.[6] but while they include specific tools for taking into account of different aspects and requirements, such as ones coming from environmental impact, the capabilities of considering more realistic structural models are still missing. In some cases statistical-based approaches are substituted by deriving structural weight prediction based on single loading parameter, like the root wing bending (see Kroo and Shevell,[7] Ning and Kroo[8]). On the other hand, specific methods based on semi-analytical approaches have been developed mainly to enhance the weight prediction capabilities (see for example Macci[9] and Bindolino et al.[10]) but in many cases they are specific modules not included into a more general aircraft conceptual design framework, including aircraft performances and stab! ility and control.

II. NeoCASS: aeroelasticity in conceptual design

Present trends in aircraft design towards augmented-stability and expanded flight envelopes call for an accurate description of the flight-dynamic behavior of the aircraft in order to properly design the Flight Control System (FCS). Hence the need to increase knowledge about stability and control (S&C) as early as possible in the aircraft development process in order to be *first-time-right* with the FCS design architecture. The starting point and inspiration for the development of a software named CEASIOM (Computerized Environment for Aircraft Synthesis and Integrated Optimization Methods), is the QCARD package for aircraft conceptual design with quasi-analytical shape definitions, aero-data correlations, and performance predictions developed by Isikveren.[11] The CEASIOM code is developed within the frame of the SimSAC[12] (Simulating Aircraft Stability And Control Characteristics for Use in Conceptual Design) Specific Targeted Research Project (STREP) approved for funding by the European Commission 6th Framework Programme on Research, Technological Development and Demonstration. The SimSAC project aims at significantly enhancing CEASIOM functionality by introducing software that initially focuses on rapid low fidelity analysis, and as appropriate, resorts to higher fidelity numerical simulations. Moreover, the code involves stability and control driven sizing and optimization earlier in the design cycle than is standard practice today. Engineers are supported in the conceptual design process of the aircraft, with emphasis on the improved prediction of stability and control properties achieved by higher-fidelity methods than found in contemporary aircraft design tools. CEASIOM integrates into one application the main design disciplines, i.e. aerodynamics, structures, and flight dynamics, impacting on the aircraft performance (see Figure 1). It is thus a tri-disciplinary analysis brought to bear on the design of the aero-servoelastic aircraft. However, the entire conceptual design process is not carried out. The framework requires as input an initial layout as the baseline configuration that is then refined and output as the revised layout. In doing this, CEASIOM, through its simulation modules, generates significant knowledge about the design in the performance, loads, and stability and control databases. An overview of the whole framewok and its architecture is reported in Von Kaenel et al.[13]

In particular, the need of aeroelastic analysis within SimSAC has led to the development of a completely new module called NeoCASS (Next Generation Conceptual Aero-Structural Sizing Suite) to perform struc-

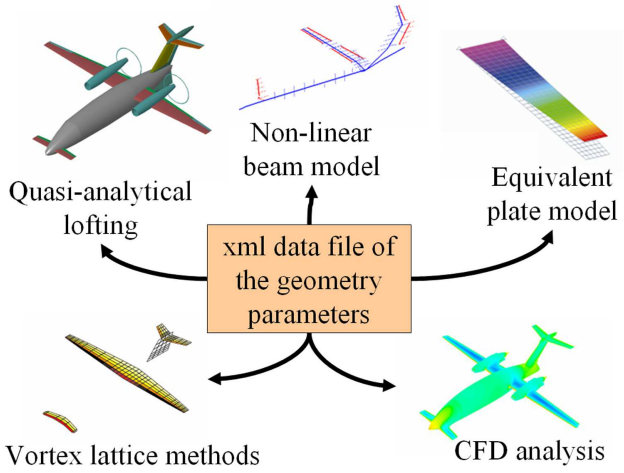

Figure 1. Geometry centric conceptual design.

tural sizing, aeroelastic analysis and optimization.
NeoCASS is compounded by three different tools:

- Weight and Balance (WB) to have a prediction of non-structural masses and their location mainly based on statistical handbooks (see Section III);
- GUESS (Generic Unknowns Estimator in Structural Sizing) to have a first guess analytical sizing of the airframe based on ultimate loads estimated on simple structural principles, one-dimensional aerodynamics and inertia distribution predicted by WB (see Section IV);
- SMARTCAD (Simplified Models for Aeroelasticity in Conceptual Aircraft Design) which is the numeric kernel for aero-structural analysis and optimization and can be used to enhance the solution provided by GUESS (see Section V).

All the sub-modules can be combined sequentially or used as stand-alone applications, providing data to different applications. For example, running through WB, GUESS and SMARTCAD it is possible to give a low to high fidelity estimation of inertia to the flight mechanics solvers. On the other hand, once an input structural model is available, SMARTCAD can enhance the aerodynamic database of the aircraft with trimmed polars and corrections to aerodynamic derivatives for different flight regimes.

Geometry handling is managed by the CADac module, developed by The Royal Institute of Technology (KTH) and outlined in Bérard et al.[14] CADac adopts a set of geometrical parameters which are general enough to ensure that a wide array of aircraft morphologies can be represented and analyzed. It also allows to estimate the room available for the airframe to be designed and all the internal-external volumes and surfaces.
Figure 2 shows a sample of some geometries that can be modeled ranging from large transport to small regional aircraft and illustrates the versatility of the geometry module.
An aircraft design geometry is fully described in a unique parametrization based on the *Extensible Markup Language* (XML) format to which all different analysis modules refer. This format allows storing each component of the aircraft and its parameter in a hierarchical and sorted way. It facilitates the sharing of data as well as the expansion of the dataset, i.e. the number of components of the aircraft can be expanded at will and it is possible to introduce new components as well as new parameters, thus increasing the range of morphologies that can be modeled. The XML format is used by most modules compounding CEASIOM, NeoCASS included, to store and manage data-transfer. This allows a high level of flexibility in updating and expanding each local database and guarantees a common format is used within the whole design framework. Furthermore, dedicated pieces of software (filter, converters, parsers) can be adopted to ease the management of such databases.
As depicted in Figure 3, geometry parameters together with geometry derived variables, e.g. area, mean chord, leading edge, quarter chord sweep, are given in the *aircraft.xml* file to:

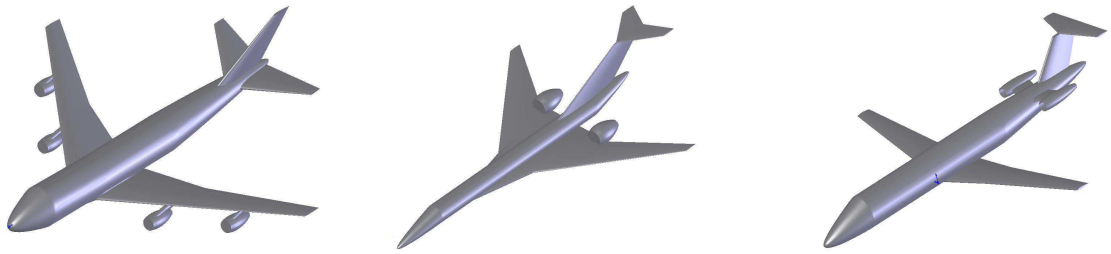

(a) Boeing 747-100. (b) Transonic cruiser. (c) Regional turbofan.

Figure 2. Sample of parametric geometry models.

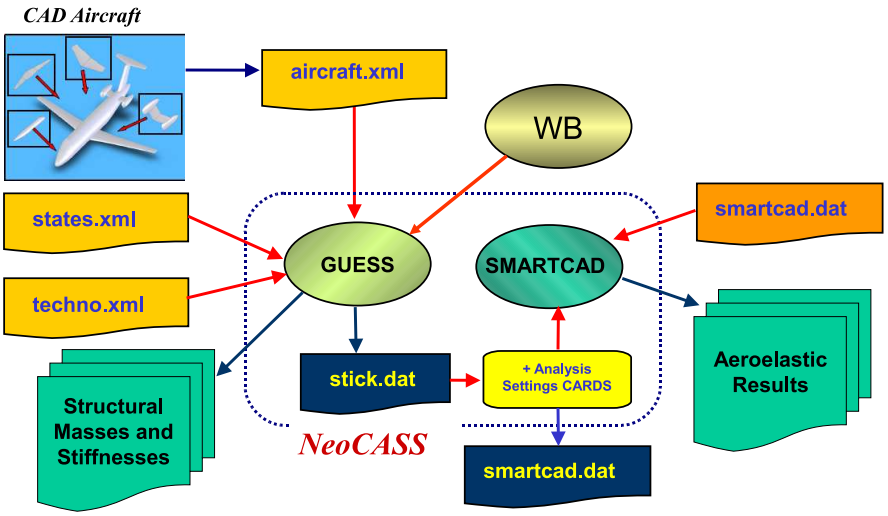

Figure 3. NeoCASS layout.

- WB which directly applies statistical formulas relying on common geometry variables;
- GUESS which generates a structural stick model, performs the sizing and generates a Finite-Element (FE) mesh;
- all other modules within the framework requiring geometry information, e.g. CAD engines, automatic mesh generators for CFD calculations.

Specific flight points chosen by the designer are given in the file *states.xml* and directly used as ultimated load conditions by GUESS to perform the first sizing. Structural concepts (see Section IV) and material properties adopted for modelling fuselage and lifting surfaces components when performing the sizing are given in the *techno.xml* file. After the sizing process, a first estimate of the structural weight and stiffness distribution is available. A stick mesh model with all elements connectivity, material properties, non-structural lumped masses coming from WB such as painting, furniture, payload, is exported to the ASCII file *stick.dat* to be used by the solver SMARTCAD for aero-structural analyses. Further parameters are provided as setting cards to the solver to determine and rule the analysis to be carried out. When the parameters are combined to the mesh file, a *smartcad.dat* file is available which can be independently re-used and modified by the designer to carry out the simulation required using SMARTCAD as a stand-alone application. Several outputs are finally available to the structural engineer for post-processing purposes, e.g. stresses, displacements, and to the other modules, e.g. stability derivatives, trimmed polars, vibration modes for flight-dynamic simulations

including aeroelastic effects, under the hypothesis of small structural displacements.

III. Weight and balance semi-empirical estimation (WB)

Once an appropriate geometry description has been defined, the next step is to be able to get a first estimation of weight and balance. At conceptual stage, aircraft weight estimation is not a trivial task, especially if new unconventional design are investigated: lack of data and continuous design changes are two main issues a designer has to face. Many aeronautical common approaches like Raymer's[1] or Torenbeek's[2] rely on semi-empirical formulas and need extensive table to search and set correction coefficients, making process automating uneasy.
The weights of the different aircraft components can be classified in three principal groups:

1. those directly related to Maximum Take-Off Weight (MTOW), i.e. wing, tail and fuselage weight;
2. fixed equipment, function only of passengers accommodation and held constant;
3. fuel and payload weights.

These three groups concur to the final MTOW by means of an iterative method: a user's defined fuel amount acts as control variable on the process leading to the minimum MTOW that fulfills airframe strength requirements at a fixed payload. Of course several payload configurations can be analyzed together with estimating the Green Manufacturer's Empty Weight (MEW). MEW and MTOW configurations define center of gravity range limits, since the former is the airframe weight comprising also propulsion, furnishing, miscellaneous contributions and any manufacturer's tolerances but without fuel and payload, while the latter is the maximum take-off weight at brake release.

Following this classification, the input set is restricted to external geometry data, such as span or fuselage length, and a few internal layout information, i.e. cabin length, fuel and payload, which includes passengers, crew and baggage (design specifications). It should be noted that statistical formula validity is not universal and their accuracy may vary, depending on the design under consideration. Nevertheless, the main target of WB is a first reasonable estimate of structural and non-structural items which will be later refined by the structural sizing and eventually by the optimization framework. Arms calculation, either for external or internal geometry, is made using volume information relying on the analytical approximation by CADac. Concentrated masses are also considered separately: if available, additional data such as such APU's (Auxiliary Power Unit) weight or auxiliary fuel tank capacity and position can be specified directly, improving the accuracy and realism of the weight prediction. A key factor for weight calculation is the maximum fuel value (and its distribution in the different tanks) that is a required user input; as for internal layout, with the exception of cabin extent (which although can be roughly estimated in 70%-80% of fuselage length), the required data can be automatically estimated by WB from statistical and semi-empirical methods.

A dedicated routine calculates inertia matrix using either a coarse approximation, which treats the whole aircraft as solid with constant density (thus using simple formulas with some correction coefficient, an example can be found in Raymer[1]), or a refined method based on the Mitchell code.[15] Both methods result in approximations, giving a first estimate of the inertia matrix that will be necessarily refined by GUESS and SMARTCAD.

IV. Analytical structural sizing (GUESS)

A method based on fundamental structural principles for estimating the load-bearing airframe for fuselage and lifting surfaces is adopted. The same approach is used within the conceptual design framework presented in Perez et al.[16] in order to have an estimate of the structural weight for a multidisciplinary optimization of an isolated wing. This method is particularly useful in the preliminary weight estimation of aircraft since it represents a compromise between the rapid assessment of component weight using empirical methods, based on actual weights of existing aircraft, and detailed but time-consuming finite-element analysis. Both methods have particular advantages but also limitations which make them not completely suitable for the conceptual design phase. The empirical approach is the simplest weight estimation tool, which requires the knowledge of fuselage and wing weights from a number of similar existing aircraft in order to produce a linear regression useful to derive the data required for the aircraft to be designed. Obviously, the accuracy of this method depends upon the quality and quantity of available data for existing aircraft and how much

closely the aircraft under investigation matches them. Thus, this approach is inappropriate for studies of unconventional aircraft concepts for two reasons:

- since the weight estimating formulas are based on existing aircraft, their application to unconventional configuration (i.e., canard aircraft) is suspect;
- the impact of advanced technologies and materials (i.e., advanced composite laminates) cannot be assessed in a straightforward way.

Continuum structures, as fuselages or wings, which would use some combination of solid, flat plate or shell finite elements, are not easily discretizable and the solution of even a moderately complex model like an aircraft is computationally intensive and can become a bottleneck in the vehicle synthesis.
Finite-element methods, commonly used in aircraft detailed design, are not appropriate for conceptual design, as the idealized structure model must be built off-line and many details are missing in such a premature phase. The following two approaches which may simplify the finite-element model also have drawbacks. The first aims at creating detailed analysis models at a few critical locations on the fuselage and wing, to successively extrapolate the results to the entire aircraft. This approach can be misleading because of the great variety of structural, load and geometric characteristics in a typical design.
The second approach aims instead to creating a coarse model of the aircraft, but this scheme may miss key loading and stress concentrations.

An alternative intermediate approach exists and it is based on beam theory. The work was originally performed by Ardema et al.[17] and presented as structural sizing tool for fuselage and wing. The method results in a weight estimate which is directly driven by material properties, load conditions, and vehicle size and shape, considering classic failure modes of each structural component involved as outlined below, thus being not confined to an existing data base.

The present work starts from this approach, extending it to the sizing of horizontal and vertical tail planes to have a complete view of the whole airframe. The distribution of loads and vehicle geometry is accounted for, since the analysis is done station-by-station along the vehicle longitudinal axis and along the lifting surface structural chord, giving an integrated weight which depends on local conditions. Classic hypothesis on inertia distribution according to local amount of volume are considered combined with one-dimensional aerodynamic analytical load distribution.
Figure 4 briefly outlines the steps involved to analytically determine the overall weight of the airframe.

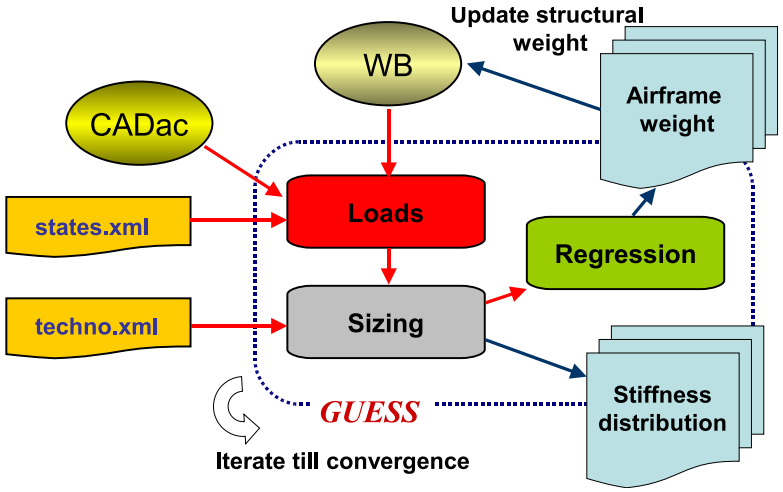

Figure 4. Layout of the analytical structural sizing tool.

The Loads and Sizing modules are the main components in the process. They respectively determine the ultimate loads and load-bearing material distribution starting from the geometry description of the airframe, maximum load factors allowed, structural concepts adopted (see Tables 1 and 2) and constraints on minimum gage.

Nevertheless, an analysis based solely on fundamental principles will give an accurate estimate of structural weight only. Thus, weights for fuselage and lifting surfaces secondary structure (including control surfaces and leading and trailing edges) and items from primary structure (such as doublers, cutouts and

K_{con}	**Structural concept**	**Best performance/ compromise**
1	Simply stiffened shell, frames	minimum weight in buckling
2	Z-stiffened shell, frames	best buckling
3	Z-stiffened shell, frames	buckling, min. gage
4	Z-stiffened shell, frames	buckling, pressure
5	Truss-core sandwich, frames	best buckling
6	Truss-core sandwich, no frames	best buckling
7	Truss-core sandwich, no frames	buckling, minimum gage, pressure

Table 1. Fuselage structural concepts

K_{con}	**Covers**	**Webs**
1	Unstiffened	Truss
2	Unstiffened	Unflanged
3	Unstiffened	Z-stiffened
4	Truss	Truss
5	Truss	Unflanged
6	Truss	Z-stiffened

Table 2. Wing-box structural concepts

fasteners) must be estimated by a correlation to existing aircraft. The initial predictions of airframe weight by WB are overwritten with the ones coming from GUESS, supposing them as more accurate. Finally, an iterative loop is performed until convergence on the structural weight.

IV.A. Sizing process

GUESS determines the distribution of stiffness and non-structural mass of the airframe subjected to different types of maneuvers such as pull-up at prescribed normal load, landing, bump on irregular runway, and rudder maximum deflection. These maneuvers can be easily prescribed by the user depending on the design specifications (for example maximum load factor, landing sink velocity, differential pressure inside the fuselage). Specific lateral maneuvers according to FAR-25 criteria are considered to improve the accuracy of vertical tail sizing, i.e. abrupt rudder maneuvers and engine-out sideslip flight. To estimate some of the key lateral directional analysis, including stability and control derivatives for use in estimating aircraft characteristics, the approach proposed by Mason[18] is adopted.
Once the loads are defined, the sizing is performed for each station under the constraints of ultimate compressive and tensile strength, local and global buckling and minimum gage.

Fuselage is idealized as slender beam with large fineness ratios, whose sizing is predominantly governed by bending loads. Usually, typical vehicles considered feature integrally stiffened shells stabilized by ring frames. In the buckling analysis of these structures, the shell is usually analyzed as a wide column and the frames are sized by the *Shanley* criterion[19] as depicted in Figure 5(a). This is the approach reported also in the book by Niu.[20] The general instability criterion is:

$$C_f = \frac{(E\,J)_f\ L}{M_u\,D^2} \tag{1}$$

where C_f is the Shanley's constant, $(E\,J)_f$ is the effective frame stiffness, D the diameter, M the ultimate bending moment and L the frame spacing. Experimental tests show that general type of instability when C_f is relatively low and that panel type of instability occurs when C_f is relatively high. The typical threshold value is $\frac{1}{16.000}$ where the occurrence of the two failure has the same probability, neglecting imperfections. Usually, C_f is nearly constant for any given cross-section shape and it does not contain any information regarding the sheet-stringer combination, thus allowing sizing the frame independently. In order to easily introduce the weight of each frame, the efficiency factor K_f given by the ratio of the moment of inertia J_f and the cross area of the frame A_f, is introduced, i.e. $K_f = \frac{J_f}{A_f}$. This parameter depends on the chosen type of section for the frame and clearly affects the proportion of the stiffened frame in terms of optimal frame spacing and frame overall weight (see the book by Shanley,[19] Chapter 4 for an example).

As for lifting surfaces, a multi web box beam (see Figure 5(b)) with the webs running in the direction of structural semispan is adopted.
As outlined in Shanley,[19] when the loading intensity is high, as in very thin or highly-loaded wings, the sheet thickness may become great enough to permit the elimination of the stringers, provided that the unsupported width of the plate is reduced by means of spanwise members. This type of construction is not only the most efficient under such conditions, but also has many advantages such as simplicity, ease of production, surface smoothness and increased stiffness. Nevertheless in this stage, a sensible distribution of stiffness and inertia is required, being the details on the section of secondary importance.
The typical structural box has width B, given a section of chord-length C. The spanwise separators have a uniform chord-spacing b and thickness t_w while the sheet thickness is t_s. Both thicknesses t_w and t_s are

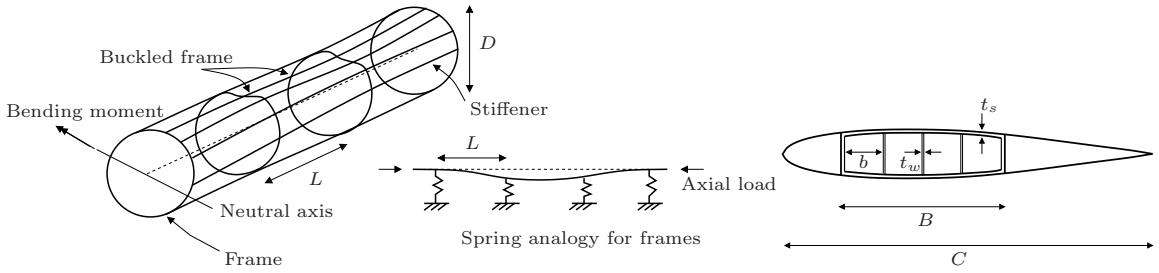

(a) General instability for framed fuselage (b) Multi-web concept

Figure 5. Structural concepts used by GUESS.

assumed as constant over the chord but vary spanwise. The same happens for the spacing b which varies spanwise, usually becoming smaller when the tip is approached. Although no ribs are needed for support of the compression surface, a minimum of two end ribs are required to maintain the airfoil contour and to complete the torsion box. Nevertheless, ribs are indeed not taken into account in this model, despite they may be needed where large concentrated loads are applied. Moreover, their contribution to the primary overall structural weight is neglected. The beam is designed by spanwise bending and shear. The cover and the webs are sized in order to prevent the critical instability mode for multi-web box beams which is characterized by simultaneous buckling of the covers and of the webs due respectively to local instability and flexure induced crushing.

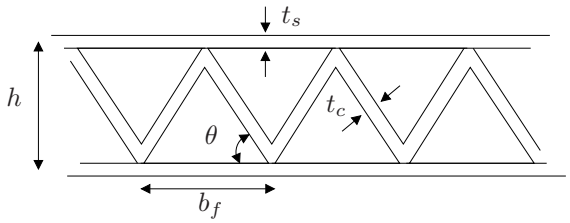

(a) Truss-core sandwich

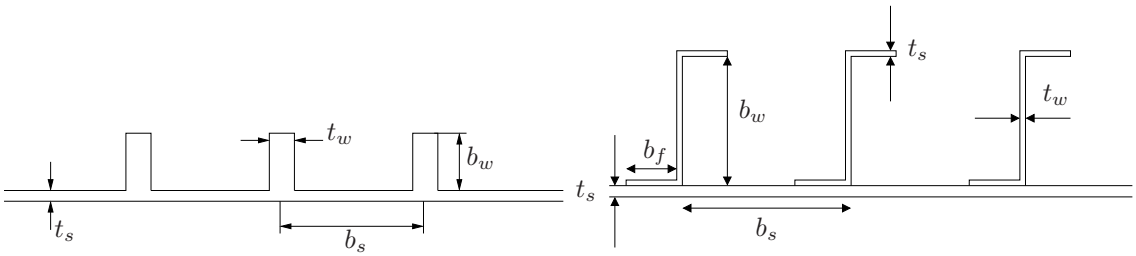

(b) Unflanged, integrally stiffened shell (c) Z-stiffened shell

Figure 6. Structural concepts adopted.

Tables 1 and 2 reports the different concepts of stiffened shells available whose primary components are depicted in Figure 6. At this stage, the goal of the structures engineer is to have available a mean of evaluating many structurally optimized cross sections together with their respective cost-producibility fabricability values. This would greatly facilitate early selection of a minimum number of candidate configurations in preliminary design situations, and narrow the focus of follow-on efforts to only those concepts that can reasonably be expected to result in an optimum design.

Principles of minimum weight can then be used such that, given an applied load and the limitations on the outside dimensions, the most efficient type of construction, its geometry and material are directly determined. Usually, these criteria are applied to the optimum design of classic structural elements such as columns, plates and composite structures, i.e. box beams and cylinders. The work by Gerard[21] is an historical review and assessment worth being mentioned, where a detailed and comprehensive bibliography on optimum structural design is critically reviewed. Significant advances in the literature of those years concerning analytical optimum design for various components, materials and thermal protection systems is

also given.

In order to afford a sound basis for weight prediction, the factors controlling the *minimum weight*, e.g. material adopted, cross-section geometry and its proportions, must be identified and combined into formulas or charts to be directly used as guidelines in sizing without actually designing the structure. For optimum structural design, the required strength is determined through *structural indexes*. Generally speaking, global and local buckling equations are combined for each element depicted in Figure 6, resulting in an *efficiency equation*, relating the *loading material index*, expressing the loading intensity divided by a specified dimension and Young modulus, to the *weight index*, given by the ratio of the equivalent thickness and the previously introduced dimension, through the *efficiency index*. This last is usually a function of geometric proportions (usually thickness ratios) and has to be maximized to have minimum weight. Having the dimensions of a stress, it directly measures the loading intensity, allowing for the application of the principles of dimensional similarity, shrinking and enlarging a-priori optimized proportions. Indeed, design proportions that are optimum for a particular structure are also optimum for structure of any size, provided they all have the same structural index. Such indexes have been developed for many basic structural components, allowing analytical minimum weight design to be carried out for rather complex stiffened structures. Examples can be found in Shanley[19] and in the report by Crawford and Burns[22] which is the basis of the work by Ardema et al.[17] and hence of the present work.

Previous considerations lead to the optimum weight, representing the lowest value achievable. This will hardly represent the real value because of the the simplifications introduced in the modelling and secondary issues (extra stiffeners, cut-outs, joints, nontaper) which cannot be introduced in this early design phase. It is then necessary to determine the sources on *non-optimum* weight and *ad-hoc* formulas to consider such weight in a rational manner. Thus, to conclude the process and determine a new prediction of structural weight, a regression analysis is carried out. This phase enables to have an estimation of the primary and total airframe weight starting from the load-bearing weight determined analytically by GUESS. Different expressions for the relation between bearing and total structural weight are carried out by Ardema et al.[17] for classic passenger-transport aircraft.

IV.B. Finite-element aeroelastic model

At the end of the sizing process, GUESS automatically generates a stick beam model for SMARTCAD by means of a semi-monocoque method. Figure 7 shows some details of the typical model generated.

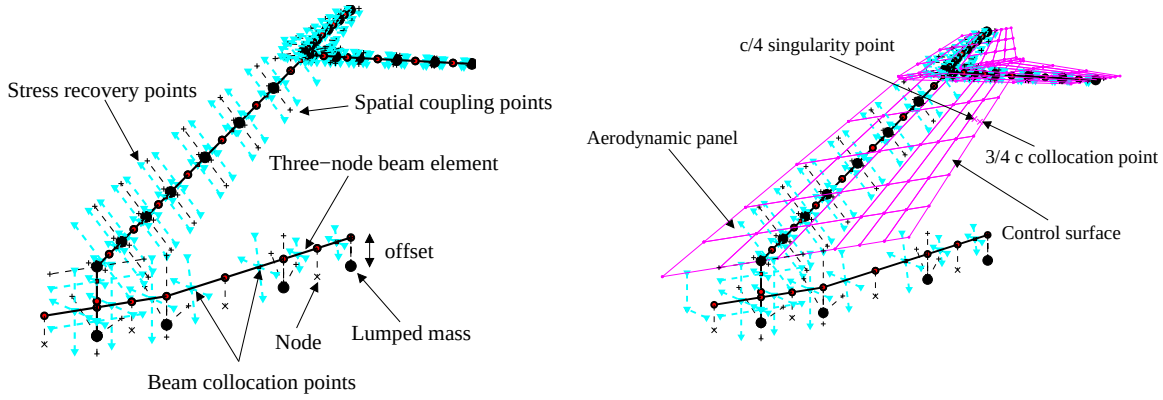

(a) Structural model

(b) Structural and aerodynamic coupled models

Figure 7. Nomenclature for the aeroelastic model.

As long as the strength requirements are fulfilled, structural flexibility is not necessarily objectionable. Aeroelastic deformations, however, may not only strongly influence the structural dynamics and flight stability, but also the overall performance and controllability of the aircraft. As introduced above, the airframe design traditionally starts with pure strength requirements since formulating and including aeroelastic requirements in the process is impractical.

Following this strategy, the first stiffness and inertial distribution determined by GUESS is used as a starting point for more detailed and specific analyses during which the airframe is assessed for several flight points and configurations by means of more refined numerical models, e.g. panel methods, finite elements.

Should deficiencies be detected, an optimal concurrent stress and repair process can be carried out through the optimization process in SMARTCAD to identify and modify areas with the most beneficial impact on stress, stiffness and aeroelastic requirements.
The main issues rely in how to transfer stiffness, inertial and aerodynamic properties. As previously mentioned, stiffness distribution are determined using simple analytical formulas starting from the bearing material estimated on each section. The two meshes may have a different discretization, thus an interpolation process of mechanical properties is carried out. This allows the designer to use a refined mesh during the analytical sizing which is a very cheap process. The discretization of the finite-element model which is certainly more time-consuming to be analyzed, is then ruled by the analyst at his own taste. Grid nodes are simply laid to form a cruciform shape and maintain the closed path of load transfer between lifting surfaces and fuselage. Thus, offsets are introduced to correctly position the elastic axis of the beam connecting the nodes which are laid so that a close connected circuit is determined, e.g. wing and vertical tail intersecting the fuselage. Besides exporting mechanical properties and the basic stick model, extra information are given:

- stress-recovery points along the sides of the wing-box and fuselage where stresses are calculated;
- extra-nodes perpendicular to the beam axis and simply connected to beam nodes through rigid elements (hyphotesis of beam model implying rigid section); they instantaneously enable to visualize the twist rotational motion of the boundaries of the wing-box and are mainly be used for the coupling with the aerodynamic model to transfer forces and displacements.

Major efforts are required to describe inertial distribution which is particularly important when the trim condition for the free-flying aircraft is sought, since a detailed description of mass values and their location is of primary importance to correctly define inertial loads. Thus, when the beam stick model is automatically generated, all non-structural masses are correctly introduced in the structural mesh as:

- lumped non-structural masses on mesh nodes (engines, landing gears, auxiliary tanks, systems);
- non-structural densities per unit length along the beams (passengers in fuselage, fuel in wings, paint, furniture).

As introduced above, these data are either provided by statistical methods or directly by the user if available. Lumped masses are easily introduced in the model by means of rigid offsets from a reference node. Beams can also be used for this purpose, but an estimation of their stiffness is required (this may happen in the case of engine pylons). For example, the non-optimum structural weight estimated by the regression method introduced above is introduced as lumped nodal masses being its chordwise position difficult to estimate in this stage. As far as distributed masses are concerned, for example fuel, the availability of an estimate of the fuel volume available in the wing-box allows to determine the mass stored for each beam along the wing-span, and thus to estimate the mass per unit length. The same approach can be applied to any distributed mass, e.g. passengers, furniture, painting and so on.

Aerodynamic mesh is represented by a a series of flat lifting boxes collecting quadrilateral panels and defined by own span, twist, dihedral and sweep. These simple tangible parameters are particularly suitable when it concerns aerodynamic shape optimization as showed in Perez et al.[16] The aerodynamic mesh created allows to be indistinguishably used for classic lifting surface panel methods such as Vortex Lattice,[23] Vortex Ring,[24] Doublet Lattice[25] and Harmonic Gradient.[26] Wing-box dimensions, internal volume of fuel available and chord-wise camber distribution are simply determined once the airfoil used at different spanwise control sections is defined. To make this feature more flexible, a user-defined airfoil library allows to include whatever airfoil the designer wants to adopt which make the tool particular suitable for simple shape-optimization once an external parametrization of the airfoil is adopted.

Considering the early design phase the framework is intended for, control surfaces are currently represented by their aerodynamic contributions, neglecting their inertia, dynamics and actuation systems. When static aeroelastic trim is sought, the analyst can specify arbitrary constraints among the control surfaces, with different gains. For example, antisymmetric ailerons deflection, symmetric elevators deflection, or wing flaps deflection can be imposed as needed. As for flutter analysis, for example, a further step would consist in the structural sizing of the control surfaces, and include a lumped static impedance to model a mechanic control-chain or to approximate the impedance of the actuators. This is currently out of the target the code is developed for and it is left to future developments.

V. Aeroelasticity in conceptual aircraft design (SMARTCAD)

SMARTCAD is the numerical module dedicated to aero-structural analysis. It can be used as a stand-alone application once the structural and aerodynamic meshes are provided, together with solver parameters. Different kind of analysis can be carried out:

- static analysis, linear buckling.
- vibration modes calculations
- linearized flutter analysis;
- linear/non-linear static aeroelastic analysis, trimmed calculation for a free-flying rigid or deformable aircraft;
- steady and unsteady aerodynamic analysis to extract derivatives for flight mechanics applications;
- structural optimization.

At the moment structural beam models and classic lifting aerodynamic surfaces are heavily used, despite the code can be coupled to high fidelity aerodynamic models belonging to the class of Computational Fluid Dynamics (CFD). Complex aeroelastic phenomena. mainly due to aerodynamic non-linearities such as the *transonic dip*, can then be investigated as outlined in Cavagna et al.[27]

The time for the preparation of the aeroelastic model is eased by the CAD-centric concept introduced above: a change in a geometry parameter is automatically reflected to the numerical model by means of automatic grid-generation which allows the whole process to be re-started for another analysis on the updated model.
In the following pages some of the components used in this work are outlined: the beam element and aerodynamic method adopted, static aeroelastic trim solution and structural optimization. Finally, an application of the whole process for a problem of static aeroelasticity is presented in Section VI.

V.A. Beam model

SMARTCAD adopts a three-node linear/non linear finite-volume beam, whose formulation was originally proposed in Ghiringhelli et al.,[28] which proved to be intrinsically shear-lock free. In this setion the main features of the formulation are outlined, focusing on the linear model which be used in the application section. The finite-volume approach leads to the collocated evaluation of internal forces and moments, as opposed to usual variational principles which require numerical integration on a one-dimensional domain. The kinematic description of the generalized deformations, the strains and the curvatures, is based on an intrinsic (kinematically exact) formulation of the beam.

As sketched in Fig. 8, each beam element is divided in three parts. Each part is related to a reference point G_i: the mid- and the two endpoints. They are referred to geometrical nodes N_i by means of offsets $\mathbf{s}_i$. This allows the elastic axis of the beam to be offset from the center of mass.
Every node is characterized by a position vector $\mathbf{x}_i$ and a rotation matrix $\mathbf{R}(\mathbf{g})$ through Gibbs-Rodrigues rotation parameters $\mathbf{g}$. A reference line $\mathbf{p}$ describes the position of an arbitrary point $\mathbf{p}(\epsilon_i)$ on the beam section.

Independent parabolic shape functions are used to interpolate displacements and rotation parameters of the generic point $\mathbf{p}(\mathbf{x}_i)$ as functions of those of the reference nodes. The derivatives of the displacements and the rotation parameters at the two collocation points C_j are used to evaluate the strains $\boldsymbol{\varepsilon}$ and the elastic curvatures $\mathbf{k}$ which are then used to compute the internal forces and moments, balancing the external forces $\mathbf{t}_i$ and moments $\mathbf{m}_i$. Collocation points are laid at $\epsilon_i = \pm\, 1/\sqrt{3}$ to recover the exact static solution for a beam loaded at the end points, as showed in Masarati and Mantegazza.[29]
Being the position of the ith node $\mathbf{p}_i = \mathbf{x}_i + \mathbf{R}\mathbf{s}_i$, the position of an arbitrary point of the reference line is interpolated by means of parabolic shape functions $\mathbf{N}(\epsilon) = \begin{pmatrix} 1/2\epsilon(\epsilon-1) & 1-\epsilon^2 & 1/2\epsilon(\epsilon+1) \end{pmatrix}$ as:

$$\mathbf{p}(\epsilon) = \mathbf{N}_i(\epsilon)\left(\mathbf{x}_i + \mathbf{R}_i\left(\mathbf{g}(\epsilon)\right)\mathbf{s}_i\right) \quad \text{with } \mathbf{g}(\epsilon) = \mathbf{N}_i\mathbf{g}_i \tag{2}$$

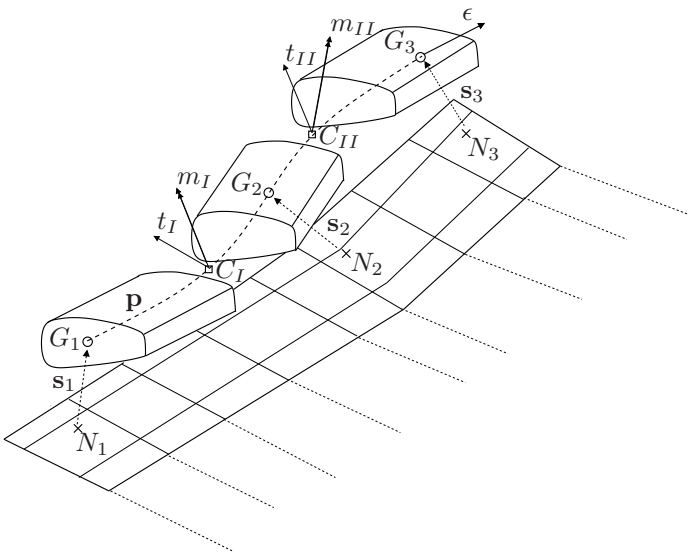

Figure 8. Finite Volume three-node beam coupled to a classic lifting surface method.

Equilibrium for each node, considering external nodal forces and internal forces at each collocation point, leads to $\mathcal{A}\Theta = \mathcal{F}$ with:

$$\mathcal{A} = \begin{bmatrix} -\mathbf{I} & \mathbf{0} & \mathbf{0} & \mathbf{0} \\ -(\mathbf{p}_I - \mathbf{p}_1)_\times & -\mathbf{I} & \mathbf{0} & \mathbf{0} \\ \mathbf{I} & \mathbf{0} & -\mathbf{I} & \mathbf{0} \\ (\mathbf{p}_I - \mathbf{p}_1)_\times & \mathbf{I} & (\mathbf{p}_{II} - \mathbf{p}_2)_\times & -\mathbf{I} \\ \mathbf{0} & \mathbf{0} & -\mathbf{I} & \mathbf{0} \\ \mathbf{0} & \mathbf{0} & (\mathbf{p}_{II} - \mathbf{p}_3)_\times & \mathbf{I} \end{bmatrix}, \quad \Theta = \begin{Bmatrix} \mathbf{f}_I \\ \mathbf{m}_I \\ \mathbf{f}_{II} \\ \mathbf{m}_{II} \end{Bmatrix}, \quad \mathcal{F} = \begin{Bmatrix} \mathbf{f}_1 \\ \mathbf{m}_1 + \mathbf{s}_{1\times}\mathbf{f}_1 \\ \mathbf{f}_2 \\ \mathbf{m}_2 + \mathbf{s}_{2\times}\mathbf{f}_2 \\ \mathbf{f}_3 \\ \mathbf{m}_3 + \mathbf{s}_{3\times}\mathbf{f}_3 \end{Bmatrix} \tag{3}$$

The matrix $\mathcal{A}$ is referred as *moment arm matrix* and depends on the current deformed shape, Θ is the vector of internal generalized forces and $\mathcal{F}$ is the vector of external generalized nodal forces. In the previous expression, the term $(\cdot)_\times$ represent the vector product matrix, i.e. if $\mathbf{a}$ and $\mathbf{b}$ are two vectors, $\mathbf{a}_\times$ is the matrix that multiplied by $\mathbf{b}$ gives $\mathbf{a} \times \mathbf{b}$, and $\mathbf{I}$ is the identity matrix.
Internal generalized forces Θ_i at each collocation point are recovered from the local reference material frame as:

$$\begin{Bmatrix} \mathbf{f}_i \\ \mathbf{m}_i \end{Bmatrix} = \begin{bmatrix} \mathbf{R}_i & \mathbf{0} \\ \mathbf{0} & \mathbf{R}_i \end{bmatrix} \begin{Bmatrix} \tilde{\mathbf{f}}_i \\ \tilde{\mathbf{m}}_i \end{Bmatrix} \quad \text{with } i = I, II \tag{4}$$

with $\mathbf{R}_i = \mathbf{R}_i(\mathbf{g}_i)$ function of the rotation parameters interpolated from the three nodes of the element. and $(\tilde{\cdot})$ indicating that an entity is referred to the material frame. The previous expression can be extended to both collocation points as:

$$\Theta = \mathcal{R}\tilde{\Theta} \tag{5}$$

with $\Theta = (\mathbf{f}_I, \mathbf{m}_I, \mathbf{f}_{II}, \mathbf{m}_{II})$, $\mathcal{R} = \text{diag}\,(\mathbf{R}_I, \mathbf{R}_I, \mathbf{R}_{II}, \mathbf{R}_{II})$.
Internal forces are related to generalized strains and curvatures through an arbitrary sectional stiffness matrix at the collocation point:

$$\begin{Bmatrix} \tilde{\mathbf{f}}_i \\ \tilde{\mathbf{m}}_i \end{Bmatrix} = \begin{bmatrix} \tilde{\mathbf{D}}_{\varepsilon\varepsilon} & \tilde{\mathbf{D}}_{\varepsilon k} \\ \tilde{\mathbf{D}}_{k\varepsilon} & \tilde{\mathbf{D}}_{kk} \end{bmatrix}_i \begin{Bmatrix} \tilde{\boldsymbol{\varepsilon}}_i \\ \tilde{\mathbf{k}}_i \end{Bmatrix} \quad \text{with } i = I, II \tag{6}$$

summarized as:

$$\tilde{\Theta} = \tilde{\mathcal{D}}\tilde{\Psi} \tag{7}$$

with $\tilde{\mathcal{D}} = \text{diag}\left(\tilde{\mathbf{D}}_I, \tilde{\mathbf{D}}_{II},\right)$, $\tilde{\Psi} = \left(\tilde{\boldsymbol{\varepsilon}}_I, \tilde{\mathbf{k}}_I, \tilde{\boldsymbol{\varepsilon}}_{II}, \tilde{\mathbf{k}}_{II}\right)$.

The generalized strains are defined as the difference between the current and the initial derivatives of the reference line $\mathbf{p}(\epsilon)$ that describes the position of the beam:

$$\left\{ \begin{array}{c} \tilde{\varepsilon} \\ \tilde{\mathbf{k}} \end{array} \right\} = \left\{ \begin{array}{c} \mathbf{R}^T \mathbf{p}' - \tilde{\mathbf{p}}_0' \\ \tilde{\boldsymbol{\rho}} - \tilde{\boldsymbol{\rho}}_0 \end{array} \right\} \tag{8}$$

where $\tilde{\mathbf{p}}_0'$ is the initial configuration of the reference line and $\tilde{\boldsymbol{\rho}}_0$ is the initial geometric curvature of the undeformed beam. The geometric curvature $\tilde{\boldsymbol{\rho}}$ of the beam reference line is defined as the axial derivative of the reference frame of the beam section:

$$\tilde{\boldsymbol{\rho}} \times = \mathbf{R}^T \mathbf{R}' \tag{9}$$

Considering the linear case which will be applied in Section VI, strains and curvatures are linearized as:

$$\boldsymbol{\varepsilon} = \mathbf{p}' + \mathbf{p}_{0\times}' \boldsymbol{\varphi} = \mathbf{N}_i' \mathbf{x}_i + \mathbf{p}_{0\times}' \mathbf{N}_i \boldsymbol{\varphi} - \mathbf{N}_i' \mathbf{s}_{i\times} \boldsymbol{\varphi}_i \tag{10}$$

$$\mathbf{k} = \boldsymbol{\varphi}' = \mathbf{N}_i' \boldsymbol{\varphi}_i \tag{11}$$

Substituting back the previous expression, the stiffness matrix is recovered:

$$\mathcal{A}\left(\mathcal{R}\,\tilde{\mathcal{D}}\,\mathcal{R}^T\right) \left[\begin{array}{cc} \mathbf{N}_{Ii} & \left(\mathbf{p}_{0\times}' \mathbf{N}_{Ii} \boldsymbol{\varphi} - \mathbf{N}_{Ii}' \mathbf{s}_{i\times} \boldsymbol{\varphi}_i\right) \\ \mathbf{0} & \mathbf{N}_{Ii}' \\ \mathbf{N}_{IIi} & \left(\mathbf{p}_{0\times}' \mathbf{N}_{IIi} \boldsymbol{\varphi} - \mathbf{N}_{IIi}' \mathbf{s}_{i\times} \boldsymbol{\varphi}_i\right) \\ \mathbf{0} & \mathbf{N}_{IIi}' \end{array} \right] \left\{ \begin{array}{c} \mathbf{x}_i \\ \boldsymbol{\varphi}_i \end{array} \right\} = \mathcal{F} \tag{12}$$

All the other matrices are evaluated in the reference configuration and do not participate to the linearization. The formulation leads to a loss of symmetry of the stiffness matrix. This is not a major issue considering that:

- usually the models are quite small and the computational cost is very limited; thus the adoption of algorithms specifically suited for symmetric problems are not of primary importance despite algorithms working with sparse matrices are recommended;
- when dealing with linearized aeroelastic problems the symmetry is always lost since the resulting aerodynamic matrices summing up to structural terms are never symmetric (see Section V.C).

Finally lumped mass matrix is created for each of the three sectors along the beam.

V.B. Low-fidelity aerodynamic models

Two low-fidelity aerodynamic methods are available in SMARTCAD, depending on whether steady or unsteady analysis is carried out:

- Vortex Lattice Method (VLM)[23] with camber contribution on normalwash once the airfoil description is provided;
- Doublet Lattice Method (DLM)[25] for the prediction of the generalized forces due to harmonic motion in the subsonic regime.

Both methods are based on potential flow theory leading, under the hypothesis of irrotational, isoentropic and inviscid flow to a Laplace's equation respectively for the linearized velocity or acceleration potential. They are certainly the most common tools adopted in aerodynamic loads prediction in the conceptual/preliminary phase (see Kier[30] for some examples in flight-mechanics applications).

By virtue of the model-linearity allowing superimposition, approximate solutions are obtained by idealizing the surface as a set of interfering elementary singularities, e.g. vortex lines and doublets, each of them satisfying Laplace's equation. Because the loading is approximated by discrete lifting elements, the method permits straightforward analyses of nonplanar and interfering configurations. The same geometric discretization of the aerodynamic surfaces as a flat lifting surface with singularities and collocation points located respectively at $\frac{1}{4}$ and $\frac{3}{4}$ of each panel chord so that Kutta condition is satisfied a priori. Thus, the same mesh is used (see Fig. 7(b)), with the only exception that the VLM takes into account camber contributions through boundary conditions and requires trailing vortexes for wake modelling. Figure 9 shows two

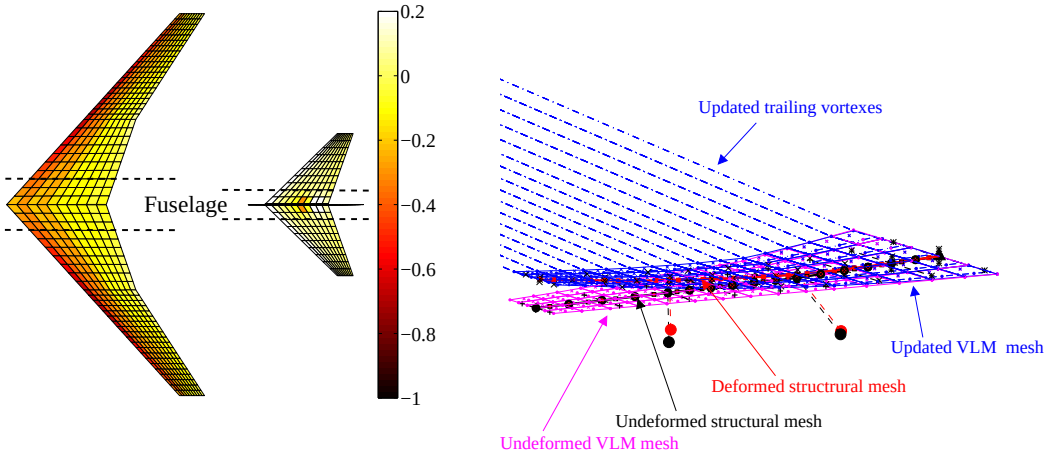

(a) Vortex Lattice (b) Clamped wing, lattice updated

Figure 9. Application of the Vortex lattice method.

example concerning the VLM; a rigid case and a case of non-linear trim where the whole lattice is updated and combined to the non-linear beam model to consider geometric non-linear effects.

Finally, an interface scheme to exchange displacements and loads between the structural grid and the aerodynamic boundary surface is required. In this specific case, the beam model represent a one-dimensional domain where the real structural geometry is hidden. On the other hand, the aerodynamic lifting surface is reduced to a two-dimensional domain. As a consequence, two radically different representations of the same aircraft geometry must be made compatible in order to transfer information between them. This is a well known problem, deeply investigated in the literature; for further reference, see Smith et al.[31,32] Two class of methods are available for this purpose within SMARTCAD: an innovative scheme, based on Moving Least Square (MLS) method (see Quaranta et al.[33]) and the Radial Basis Function (RBF) method (see Beckert and Wendland,[34] Schaback and Wendland[35]). Both methods ensure the conservation energy transfer between the fluid and the structure and they are suitable for the treatment of complex configurations. To avoid interpolating rotations and using the same algorithms in a straightforward way also for CFD meshes, extra points are added along the wingbox through rigid-arms. Aerodynamic loads are distributed along both master beam nodes and these additional nodes. Loads are then reduced to lumped forces and moments on the former set of nodes.

V.C. Static linear aeroelasticity

Considering a generic point can undergo a motion given by the sum of rigid and elastic deformable shape functions, i.e. $\mathbf{u} = \mathbf{\Phi}_R\,\mathbf{q}_R + \mathbf{\Phi}_E\,\mathbf{q}_E$, the general equation governing the dynamic of the flying deformable aircraft is:

$$\mathbf{M}\ddot{\mathbf{q}} + \mathbf{C}\dot{\mathbf{q}} + \mathbf{K}\mathbf{q} = \mathbf{Q}_0 - (\mathbf{M}_c\ddot{\mathbf{q}}_c + \mathbf{C}_c\dot{\mathbf{q}}_c + \mathbf{K}_c\mathbf{q}_c) \tag{13}$$

where $\mathbf{M}$, $\mathbf{C}$, $\mathbf{K}$ are respectively the mass, damping and stiffness matrix of the overall system, $\mathbf{q}$ the generalized coordinates given by rigid and deformable contributions, i.e. $\mathbf{q} = (\mathbf{q}_R, \mathbf{q}_E)$, $\mathbf{Q}_0$ the vector of generalized external forces including reference aerodynamic load and $\mathbf{q}_c$ are the generalized coordinates for controls deflections, whose effects are introduced through the generalized matrices with subscript c.
The common approach in aeroelasticity considers these equations in the reference Cartesian frame with a selected origin in a point O; rigid dynamic is simply given by three translations and rotations along its axes. In this work, the elastic coordinates are directly represented by nodal generalized displacements $\mathbf{u}_E$, i.e. $\mathbf{\Phi}_E$ is the identity matrix and $\mathbf{q}_E = \mathbf{u}_E$. Linearized rigid body modes $\mathbf{\Phi}_R$ enable to recover displacements and rotations for every node from the motion of the reference point representing the gross motion of the aircraft, as:

$$\mathbf{u}_{Ri} = \mathbf{\Phi}_{Ri}\mathbf{q}_R = \begin{bmatrix}\mathbf{I} & (\mathbf{x}_P - \mathbf{x}_0)_\times\end{bmatrix}\mathbf{q}_R \tag{14}$$

with $\mathbf{x}_P - \mathbf{x}_0$ the distance between the generic ith node and the refence point O.

Adopting a quasi-steady approximation for aerodynamic forces and neglecting control surface mechanical stiffness and damping, the system of equations governing the overall motion of the aircraft and its structural response, is:

$$\begin{bmatrix} \mathbf{M}_{RR} & \mathbf{M}_{RE} \\ \mathbf{M}_{ER} & \mathbf{M}_{EE} \end{bmatrix} \begin{Bmatrix} \ddot{\mathbf{q}}_R \\ \ddot{\mathbf{q}}_E \end{Bmatrix} + \left(\begin{bmatrix} \mathbf{0}_{6\times 6} & \mathbf{0}_{6\times N_E} \\ \mathbf{0}_{N_E\times 6} & \mathbf{C}_{EE} \end{bmatrix}_S - \frac{q_\infty L_a}{V_\infty} \begin{bmatrix} \mathbf{C}_{RR} & \mathbf{C}_{RE} \\ \mathbf{C}_{ER} & \mathbf{C}_{EE} \end{bmatrix}_A \right) \begin{Bmatrix} \dot{\mathbf{q}}_R \\ \dot{\mathbf{q}}_E \end{Bmatrix} + \left(\begin{bmatrix} \mathbf{0}_{6\times 6} & \mathbf{0}_{6\times N_E} \\ \mathbf{0}_{N_E\times 6} & \mathbf{K}_{EE} \end{bmatrix}_S - q_\infty \begin{bmatrix} \mathbf{K}_{RR} & \mathbf{K}_{RE} \\ \mathbf{K}_{ER} & \mathbf{K}_{EE} \end{bmatrix}_A \right) \begin{Bmatrix} \mathbf{q}_R \\ \mathbf{q}_E \end{Bmatrix} = \begin{Bmatrix} \mathbf{Q}_{R0} \\ \mathbf{Q}_{E0} \end{Bmatrix} - \begin{bmatrix} \mathbf{M}_{Rc} \\ \mathbf{M}_{Ec} \end{bmatrix} \ddot{\mathbf{q}}_c + \frac{q_\infty L_a}{V_\infty} \begin{bmatrix} \mathbf{C}_{Rc} \\ \mathbf{C}_{Ec} \end{bmatrix}_A \dot{\mathbf{q}}_c + q_\infty \begin{bmatrix} \mathbf{K}_{Rc} \\ \mathbf{K}_{Ec} \end{bmatrix}_A \mathbf{q}_c \tag{15}$$

being L_a the reference aerodynamic chord and q_∞ and V_∞ respectively the flight dynamic pressure and velocity. Structural terms are indicated with $(\cdot)_S$ subscript while aerodynamic influence matrices with $(\cdot)_A$. The inertial coupling between $\mathbf{q}_E$ and $\mathbf{q}_R$ through $\mathbf{M}_{ER}$ and $\mathbf{M}_{RE}$ is highlighted; $\mathbf{M}_{RR}$ is the rigid body mass matrix with respect to point O, while $\mathbf{M}_{EE}$ is the mass matrix associated to elastic coordinates. Six reference conditions have to be defined in order to correctly couple the reference motion and the structural motion referred to the former (see Canavin and Likins[36] for further information). Considering a mean axes formulation, it is possible to nullify such inertial coupling, imposing the orthogonality of the structural displacement with the rigid modes through the mass matrix $\mathbf{M}_{EE}$ of the model:

$$\mathbf{\Phi}_R^T \mathbf{M}_{EE} \mathbf{\Phi}_E \mathbf{q}_E = 0 \tag{16}$$

Neglecting contributions due to $\ddot{\mathbf{q}}_E$, $\dot{\mathbf{q}}_E$ and control derivatives (the definition of static aeroelasticity), it is possible to determine the deformed shape from the second system of equations, representing structural steady equilibrium:

$$\mathbf{q}_E = \mathbf{K}_{AE}^{-1} \left(\frac{\mathbf{q}_\infty L_a}{V_\infty} \mathbf{C}_{ER_A} \dot{\mathbf{q}}_R + q_\infty \mathbf{K}_{ER_A} \mathbf{q}_R + \mathbf{Q}_{E0} + q_\infty \mathbf{K}_{Ec_A} \mathbf{q}_c \right) \tag{17}$$

with $\mathbf{K}_{AE} = \mathbf{K}_{EE_S} - q_\infty \mathbf{K}_{EE_A}$. Finally the equation governing the gross motion of the deformable aircraft is:

$$\begin{aligned} \mathbf{M}_{RR} \ddot{\mathbf{q}}_R = {} & \frac{q_\infty L_a}{V_\infty} \left(\mathbf{C}_{RR_A} + q_\infty \mathbf{K}_{RE_A} \mathbf{K}_{AE}^{-1} \mathbf{C}_{ER_A} \right) \dot{\mathbf{q}}_R + q_\infty \left(\mathbf{K}_{RR_A} + q_\infty \mathbf{K}_{RE_A} \mathbf{K}_{AE}^{-1} \mathbf{K}_{ER_A} \right) \mathbf{q}_R \\ & q_\infty \left(\mathbf{K}_{Rc_A} + q_\infty \mathbf{K}_{RE_A} \mathbf{K}_{AE}^{-1} \mathbf{K}_{Ec_A} \right) \mathbf{q}_c + \left(\mathbf{Q}_{R0} + q_\infty \mathbf{K}_{RE_A} \mathbf{K}_{AE}^{-1} \mathbf{K}_{ER_A} \mathbf{Q}_{E0} \right) \end{aligned} \tag{18}$$

from which it is possible to see extra-aerodynamic terms sum to the ones of the rigid aircraft, referred as *corrections* to aerodynamic derivatives and the intercept is affected by structural deformability.
The final equation including aeroelastic correction in the $\tilde{(\cdot)}$ terms is:

$$\mathbf{M}_{RR} \ddot{\mathbf{q}}_R = \frac{q_\infty L_a}{V_\infty} \tilde{\mathbf{C}}_{RR_A} \dot{\mathbf{q}}_R + q_\infty \tilde{\mathbf{K}}_{RR_A} \mathbf{q}_R + q_\infty \tilde{\mathbf{K}}_{Rc_A} \mathbf{q}_c + \tilde{\mathbf{Q}}_{R0}$$

which in the most general case leads to six equations of equilibrium from which six unknowns can be determined once the remaining are defined in order to specify the maneuver to perform.

V.D. Optimization method

The optimal solution is not necessarily sought for. The minimum weight structural concepts are adopted and geometric constraints on minimum gage are imposed to avoid unfeasible optimal solutions. This fact together with stiffness and aeroelastic constraint does not necessarily lead to the global optimum solution. Nevertheless the first structural sizing on minimum weight principles according to strength criteria on ultimate loads is considered to be a good starting point for stiffness and inertia distribution. Thus, a simple optimization process based on Gradient-based Optimization Methods can be adopted to slightly modify the airframe so that aeroelastic requirements are satisfied as well (see Figure 10).

Computational design techniques are based on numerical analysis methods evaluating the merit, commonly referred as *objective function*, of a set of feasible designs. Traditionally, the process of design using

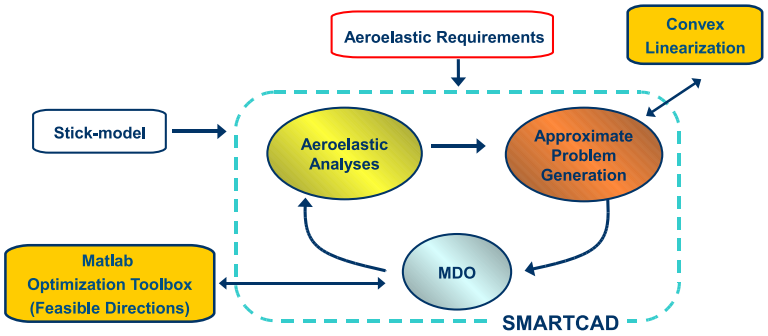

Figure 10. Optimization process within SMARTCAD.

numerical simulation has been carried out by trial and error, mainly relying on the experience and intuition of the designer in selecting the combination of the design variables. When the number of design variables increases, making correct choice may become very hard, thus to efficiently span the design space of large dimension, numerical simulations need to be combined with automatic procedures.
The classic statement for the problem of constrained optimization reads:

$$\begin{array}{lll} \text{minimize :} & I(d_j) & \\ \text{with respect to :} & d_j, & j = 1, 2, \ldots, N_d \\ \text{subject to :} & g_m(d_j) \geq 0, & m = 1, 2, \ldots, N_g \end{array}$$

where I is a non-linear function of the design variables d_j and g_m are the non-linear constraints to be satisfied. The parameters are allowed to vary in a limited design space to guarantee a feasible and realistic solution such that the design features the best figure of merit. Optimization algorithms are supposed to perform such task in a rigorous way. Many methods are available and the literature on this topic is large. A good textbook to refer is for example the one by Hatfka.[37]

A well known category is the gradient-based one which uses the value of the objective function and its gradients with respect to the design variables. The sensitivity information is used to determine iteratively the design variables $\mathbf{d}$:

$$\mathbf{d}^{n+1} = \mathbf{d}^n + \alpha^n \, \mathbf{S}^n \tag{19}$$

where n if the iteration number and α^n is the step length along the search direction $\mathbf{S}$ which assures the furthest reduction of the objective function. In the present work, the direction is defined determining the gradients and sensitivities of constraints numerically. During the optimization process, the objective and the constraints must be repeatedly evaluated, raising the overall computational cost since each evaluation demands for a numerical simulation. A common approach consists in creating an approximated linearized problem and feed the optimizer with such simplified model. This results in a very relatively inexpensive process.

Gradient-based methods converge to the optimum with significantly fewer functional evaluations than the zeroth order methods like the evolutionary ones. The disadvantage is that these methods work well with smooth objective functions, convergence to local minima is guaranteed but the optimal design could depend on the initial point. Zeroth order methods strictly rely only on the value of the objective function. When the number of design variables increases, many evaluations are required resulting in an extremely computation cost. On the other hand, in problems with a limited number of design variables with multiple local minima or discontinuities, zeroth order methods are more suitable.

To allow efficient and fast optimizations, the approach adopted here directly relyes on simplified aerodynamic and structural models, i.e. combination of beam models and lifting surfaces methods for static aeroelastic analysis. A similar approach is adopted in Osterheld et al.[38] where beam and plate models are combined with source/doublet panel methods to carry out the first structural sizing. Due to limited amount of detail within global aircraft models, the strength and buckling analysis cannot be performed based purely on finite elements methods. Thus, semi-analytical procedures are usually adopted and included in the optimization process as pursued in the present work. The same efficiency equation for minimal weight sections

are included as buckling constraints, which, generally speaking, depends by a combination of skin thickness and web thickness and spacing.

Requirements definition and quantification is for sure one of the most important phases allowing the designer to drive the optimization process and the final result. Interactions among different aeroelastic requirements exist and are not obvious to quantify. Also, since the design process is performed with a few dominating load cases, there is a risk of not meeting the design criteria for the complete set of design driving load cases. Engineering experience is extremely valuable in such task.

VI. Application to the Transonic Cruiser TCR aircraft

The whole process developed is applied to the target aircraft within the SimSAC project: the TranSonic Cruiser (TCR) whose main design specifications are summarized in Table 3. Figure 11 shows the CAD model coming from the parametric geometry module CADac. In particular, Figure 12 shows respectively the wing and the vertical fin, while Figure 13 the fuselage from two different perspectives. As it can be seen, the parametes used in the geometry module can describe successfully its complex geometry, especially when it concerns the fuselage fore and aft extremes.

Figure 11. CAD model for the TCR

Cruise Mach	0.97 at altitude$\geq$ 37.000 ft
Range	5.500 nm + 250 nm to alternate airport + 0.5 hour loiter at 1.500 ft
Max payload	22.000 Kg
Passengers	200
Crew	2 pilots, 6 cabin attendants
Take-off distance at h=2.000 ft	2.700 m at max W_{TO}
Landing distance at h=2.000 ft	2.000 m at max W_L max payload, normal reserves
Powerplant	2 turbofans
Certification	JAR25
Maneuvering load factors	2.5, -1
Max load factors	3.1, -1.7

Table 3. Design specifications for TCR

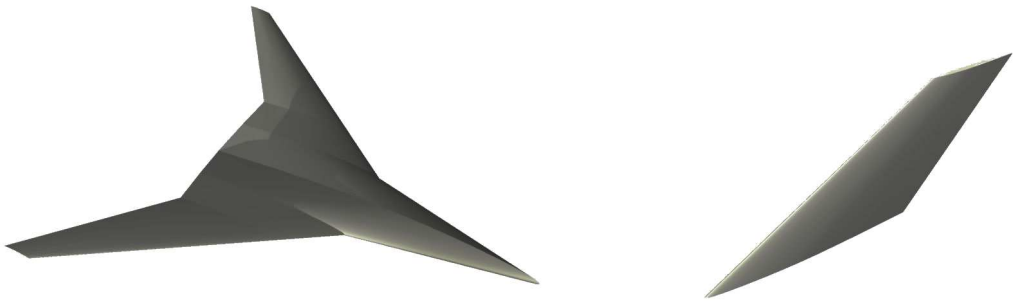

(a) Wing (b) Vertical fin

Figure 12. Wing and vertical tail CAD representation.

VI.A. Weight estimates

The first estimates determined through the WB module gives a maximum empty empty weight M_{MEW} of 128.034 Kg and a maximum take off weight M_{TOW} of 220.034 Kg (considering a total fuel weight of 92.000 Kg distributed respectively for 75% in wings and 25% in the fuselage central box). The longitudinal position

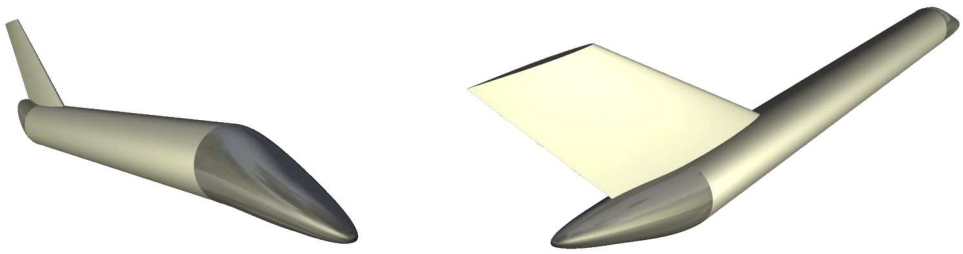

(a) Front view (b) Rear view

Figure 13. Fuselage CAD representation.

of the center of gravity with respect to the fuselage nose for the first case is $\mathbf{X}_{MEW} = [36.562, 0, -0.033]$ m, while for the second case is: $\mathbf{X}_{MTOW} = [36.389, 0, -0.30]$ m. The principal moments of inertia are $\mathbf{J}_p = [J_{xx}, J_{yy}, J_{zz}] = [9.768, 20.407, 28.242] \cdot 10^6$ Kg/m^2.
The weight of the main components are briefly summarized in Table 4 where comparisons with a similar approach by SAAB are reported. Fairly good agreement is found by both methods despite the M_{TOW} is slightly higher, the wing is slightly lighter and the tail heavier.

Component	**Mass WB** [kg]	**Mass SAAB** [kg]
Wing	24.904	21.534
Horizontal tail	1.033	1.929
Vertical tail	2.890	3.678
Landing gear	7.227	8.102
Fuselage	20.931	21.353
Powerplant	35.545	31.127
Total M_{TOW}	220.034	226.764

Table 4. TCR weight comparison with SAAB data.

VI.B. First structural sizing

The GUESS module determines the first structural sizing and generates the aeroelastic model for further structural and aeroelastic analyses. One of the main issues relies in faithfully distributing payload and non-structural masses. Representing concentrated items like engines, auxiliary tanks and landing gears by means of lumped masses rigidly attached to the main structure is straightforward. Masses are simply introduced by means of rigid arms connected to the nodes of the mesh. Figure 14 shows the stick model and the aerodynamic mesh generated. The black dots represent the lumped contributions for landing gears, engines and secondary structural masses coming from the regression analysis.

On the other hand, introducing distributed masses estimated by the WB module, e.g. fuel in the wing-box, paint, passengers, furniture weight, is more complicated because the overall weight of each item has to be properly distributed. Figure 15(a) shows the distribution of such masses along fuselage axis, whose components are smeared over a specific portion of the total fuselage length on the basis of the position of their center of gravity:

- interior, over fuselage length in proportion to beam volume;
- furniture, over fuselage length in proportion to beam volume;

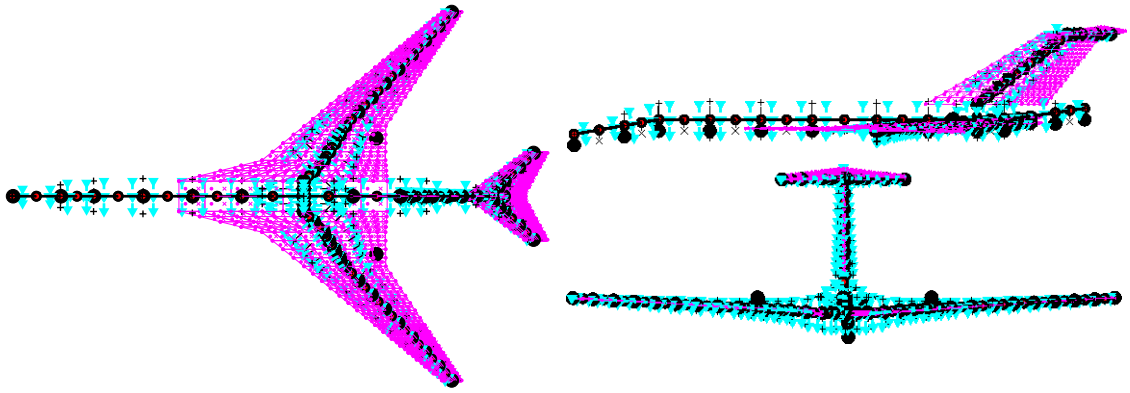

Figure 14. Aeroelastic model for the TCR aircraft.

- baggage, over passenger compartment length in proportion to beam volume;
- crew, over passenger compartment length in proportion to beam volume;
- passengers, over passenger compartment length in proportion to beam volume;
- pilots, over cockpit length in proportion to beam volume;
- paint, over fuselage length in proportion to beam wetted area.

Non-structural mass for all lifting surfaces, wing and tails, include paint weight which is distributed in proportion to the beam wetted area. No additional masses are considered for the tail planes.
For the main lifting surface, wing fuel tanks and central fuel tank are accounted for, recovering the estimations performed by WB module:

- fuel stored in wing tanks is distributed in proportion to beam volume over the cantilever wing, from wing-fuselage intersection to wing tip;
- fuel stored in central tank is uniformly distributed over the wing carrythrough structure.

Figure 15(b) represents the distribution of non-structural masses over the structural beams for the semiwing, from body center-line to wing tip.

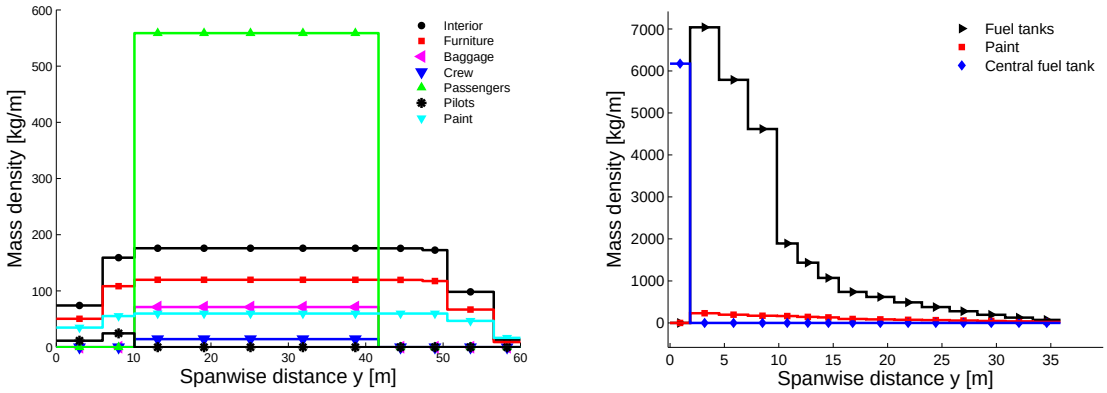

(a) Fuselage (b) Semi-wing

Figure 15. Distribution of mass linear densities for non-structural components.

The estimated weights for the fuselage are briefly summarized in Table 5. All the structural concepts available are investigated together with different values for the efficiency factor K_f concurring to the bending stiffness of the frames (only for the concepts between 1 and 5). Also, a pressure gradient $\Delta P = 13.65$ psi is considered

to show the benefits in stress relieving. The concepts 6 and 7 lead to a lower structural weight, thanks to their better buckling performance. For the concepts between 1 and 5, it is possible to note the weight estimates are fairly close, thus showing a weak dependence on the structural concept adopted. However, the discrepancy with the last two concepts can be reduced considering better performing frame section, raising the frame efficiency K_f. Finally, the values determined also have a good correspondence with the statistical prediction by WB when poor frame sections are considered ($K_f = 1$ or 2).

$\mathbf{K_{con}}$	$\mathbf{K_f = 5.24}$ [Kg]	$\mathbf{K_f = 2}$ [Kg]	$\mathbf{K_f = 1}$ [Kg]
1	5.937	6.659	7.277
2	5.356	5.924	6.241
3	5.622	6.283	6.850
4	5.671	6.318	6.888
5	6.332	7.055	7.675
6	5.207	-	-
7	5.139	-	-

$\mathbf{K_f = 2, \Delta p}$ [Kg]	$\mathbf{K_f = 5.24}$ [Kg]	$\mathbf{K_f = 2}$ [Kg]	$\mathbf{K_f = 1}$ [Kg]
16.555	15.173	17.106	18.690
14.761	13.692	15.215	16.494
15.614	14.372	16.138	17.596
15.750	14.497	16.229	17.693
17.648	16.214	18.124	19.714
13.274	13.376	-	-
12.854	13.200	-	-

Table 5. Fuselage load bearing (left) and total material (right) estimated for different parameters.

The structural weights for the main wing are reported in Table 6. Again, all the available structural concepts are used. It is possible to note the first three concepts featuring a simple unstiffened skin, lead to high structural weights if compared to the last three concepts. This is basically due to the buckling critical loads. Indeed, the last three concepts feature a better behavior in this respect since the cover is stiffened, allowing for a higher critical load. This results in a section with thinner cover (which has the major role in contributing to the weight of bearing material), thicker webs but with a higher spacing. Again, the results for the last three concepts agree fairly well with the statistical prediction by WB.

K_{con}	**Bear. material** [Kg]	**Tot. weight** [kg]
1	27.610	44.280
2	26.670	40.470
3	25.710	47.170
4	17.540	25.820
5	17.240	24.980
6	16.460	25.920

Table 6. GUESS prediction for TCR wing.

K_{con}	**VT Tot. weight** [Kg]	**HT Tot. weight** [kg]
1	7.375	2.675
2	6.337	2.498
3	8.119	3.013
4	2.454	1.632
5	2.188	1.593
6	2.618	1.568

Table 7. GUESS prediction for TCR tail.

The same trend is found when it concerns tail empennages. The stiffened cover concepts outperforms the unstiffened ones, as reported in Table 7. Again, good agreement with statistical methods is determined.

Finally, three combinations of fuselage and lifting surfaces are showed in Table 8, ranging from the two extrema of lightest and heaviest solution. They are simply determined considering the best and worst case for each component. Moreover, an intermediate solution is also reported to prove for this case the result is very close to the minimum value determined. The longitudinal position of the center of gravity is reported, together with the principal moments of inertia. Again, acceptable agreement with the statistical methods by WB is found.

VI.C. Structural analysis and optimization

In this section a simple example of optimization is considered starting from the first sizing provided by GUESS. One of the heaviest predicted cases is analyzed, considering a model with the following features:

- 11 beams for the fuselage ($K_{con} = 4$), with three design variables each: cover thickness ts_F, frame spacing d_F and frame area A_F;

$\mathbf{K}_{con}$ fuselage	$\mathbf{K}_{con}$ lifting surfaces	MTOW [Kg]	$\mathbf{X}_{CG}$ [m]	$\mathbf{J}_{xx} \cdot 10^6$ $\mathbf{Kg/m^2}$	$\mathbf{J}_{yy} \cdot 10^6$ $\mathbf{Kg/m^2}$	$\mathbf{J}_{zz} \cdot 10^6$ $\mathbf{Kg/m^2}$
7	6	211.420	37.215	7.827	18.962	25.447
4	4	212.143	37.156	7.798	19.144	25.570
5	1	240.024	37.899	9.482	23.240	30.820

Table 8. TCR M_{TOW} for different combinations of structural concepts.

- 32 beams for the wing ($K_{con} = 1$), with three design variables each: cover thickness ts_W, web spacing dw_W and web thickness tw_W;
- 12 beams for the horizontal tail ($K_{con} = 1$), with three design variables each: cover thickness ts_{HT}, web spacing dw_{HT} and web thickness tw_{HT};
- 8 beams for the vertical tail ($K_{con} = 2$), with three design variables each: cover thickness ts_{VT}, web spacing dw_{VT} and web thickness tw_{VT}.

Considering the symmetry of the model, the total number of design variables is 123. Three simple frozen maneuvers at altitude 5.000 m and $M_\infty = 0.5$ are considered:

- steady pull-up at load factor $n_z = 2.5$;
- cruise condition with a sideslip angle of 20 deg;
- snap-roll maneuver from a cruise condition with abrupt rudder and elevator deflection of 20 deg.

These maneuvers are chosen with the objective of bringing each component, i.e. wing, fuselage and tail empennages, to the limit case for bending and torsional loads.
For each beam of the model, the following constraints are considered for all the maneuvers:

- positive safety margin for normal and shear stresses;
- positive safety margin for fuselage buckling using Shanley's method;
- positive safety margin for lifting using their efficiency equation which combines cover thickness, web spacing and thickness;

resulting in 567 constraints.

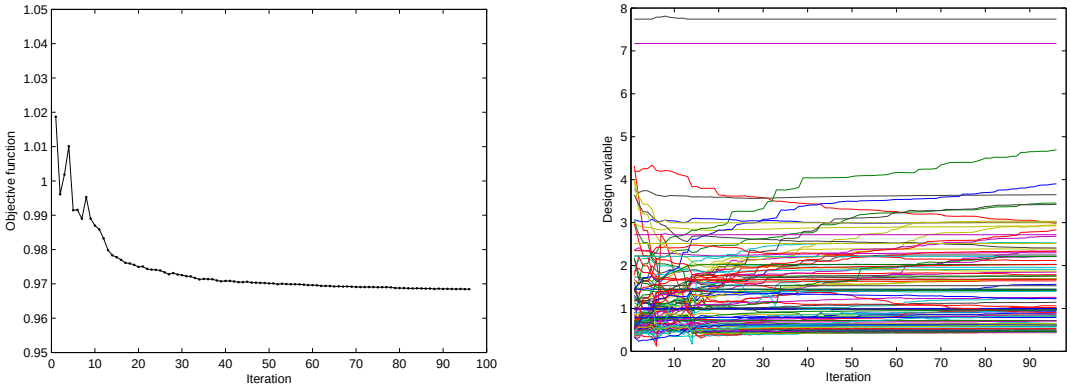

(a) Objective function (b) Design variables

Figure 16. Optimization history (all quantities normalized respect to nominal value).

The guess solution is unfeasible; due to the simplifications adopted in performing the first sizing some sections indeed result in a slightly negative safety margin.

Furthermore, design variables are have an inferior limit to determine a real feasible solutions, i.e. at least two webs for each section and minimum gage thicknesses allows for covers and webs. The objective function is rapresented by the total weight which has to be minimized.

The optimization process leads to a decrement of the total bearing material weight of approximately 3.2% of W_{MTOW}, starting from a solution of $W_{MTOW} = 236.608$ Kg.
Figure 16(a) shows the history of the objective function while Figure 16(b) gives a qualitative trend of the design variables. It can be seen the solution approaches the final value after approximately 40 iterations. All the constraints are satisfied, i.e. each section has a positive safety margin respect to yielding and buckling. An overall lightening is determined, adjusting at the same time the critical sections.
Figure 17 shows the deformed shape for the steady pull-up before and after the optimization process. The displacements at the wing-tip are higher because of the lightening, while the downward displacement for the horizontal tail is reduced thanks to a localized stiffening for the backward sections of the fuselage and the vertical-tail.

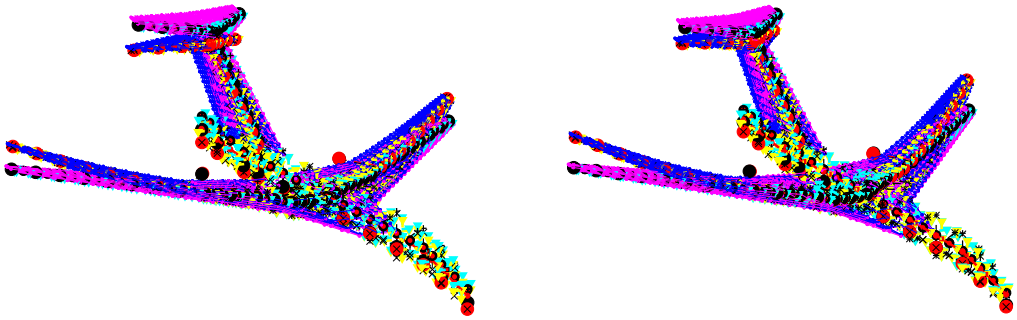

(a) Reference case (b) After optimization

Figure 17. Deformed shapes for a steady pull-up, $n_z = 2.5$ before and after the optimization.

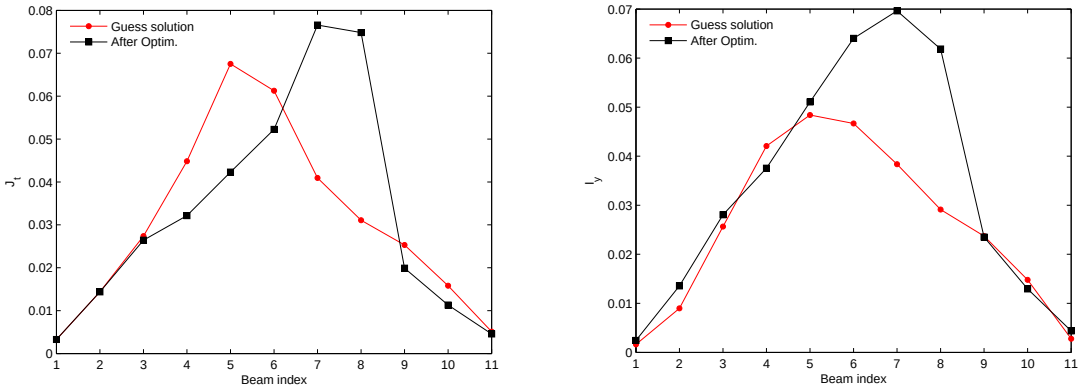

(a) Torsional constant (b) Moment of inertia (circular section)

Figure 18. Fuselage updated solution.

Indeed, Figure 18 shows the differences between the torsional constant and moment of inertia of the new solution. The sections from the carrythrough up to the intersection with the vertical tail are stiffened, resulting in raise of the aforementioned properties. The maximum peak is shifted back with respect to the reference solution simply because the GUESS module uses the aerodynamic quarter-chords as reference axis, while the stick model is correctly laid along the elastic axis.
Figure 19 outlines the new distribution of stiffness for the vertical tail. The torsional constant and out-of-plane moment of inertia are governed by the asymmetric maneuvers. The downward displacements of the horizontal tail are lowered consequently to a raise in the in-plane bending stiffness which is, on the other hand, governed by the symmetric pull-up.
Figure 20 outlines the new distribution for the wing and the carrythrough (first three beams). For this

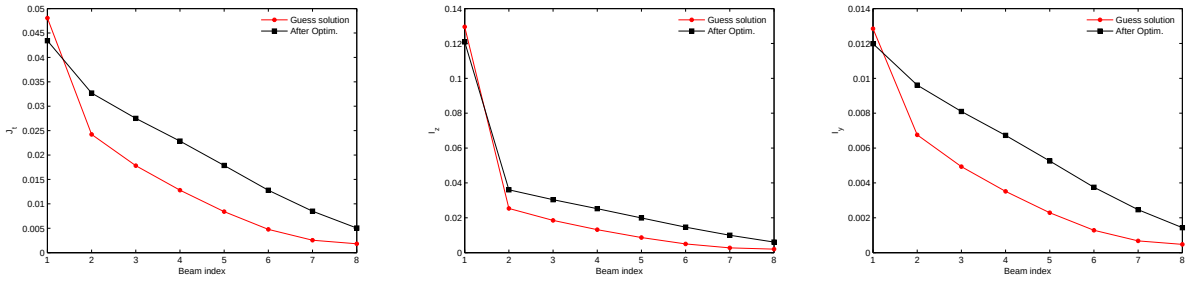

(a) Torsional constant (b) In plane moment of inertia (c) Out of plane moment of inertia

Figure 19. Vertical tail updated solution.

component the overall stiffness is reduced, which explains the overall weight saving achieved. The same happens for the horizontal tail where minor changes take place.

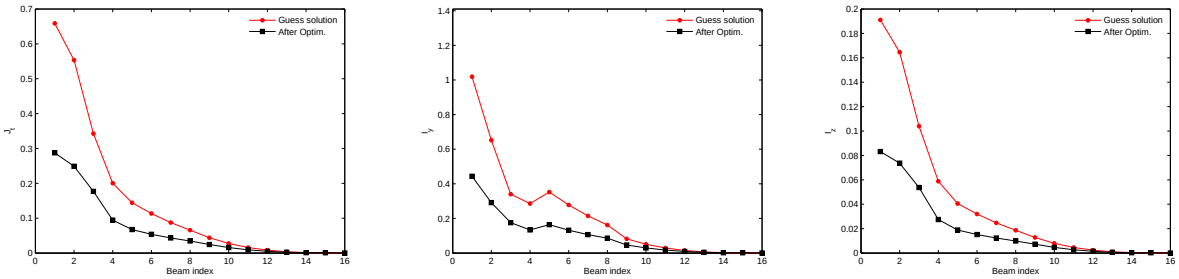

(a) Torsional constant (b) In plane moment of inertia (c) Out of plane moment of inertia

Figure 20. Wing updated solution.

The changes in some of the aerodynamic derivatives are briefly reported in Table 9. In particular, there is a reduction in the derivative associated to the aileron on the roll moment due to the lightening of the wing and the associated reduction in the torsional stiffness. On the other hand, due to a torsional stiffening of the vertical tail, the side aerodynamic derivative associated to the rudder is increased.

	Rigid	**Reference**	**After opt.**
C_z/α	3.761	3.774	3.740
C_m/α	-7.214	-7.160	-7.057
$C_l/\delta_{aileron}$	0.079	0.059	0.049
C_y/δ_{rudder}	0.158	0.079	0.101
C_l/p	-0.304	-0.297	-0.286

Table 9. Stability derivatives, $M_\infty = 0.5$, $z = 5000$ m.

In order to raise the aforementioned stability derivatives to the 75% of the rigid value, a second optimization is carried out, adding two extra constraints on $C_l/\delta_{aileron}$ and C_y/δ_{rudder}. In this case, the overall weight saving is raised respect to the previous case, resulting in an overall weight reduction of 2.62% of the W_{MTOW}. As expected, Figure 21 shows the torsional constants for the wing and the vertical tail are incremented to comply with the new constraints.

VII. Conclusion

A procedure for aero-structural conceptual design has been presented. It allows to design the airframe once the aerodynamic shape is defined relying on numerical methods and reducing to the minimum the adoption of statistics typical of this design phase. All the steps to carry out these kind of simulation have

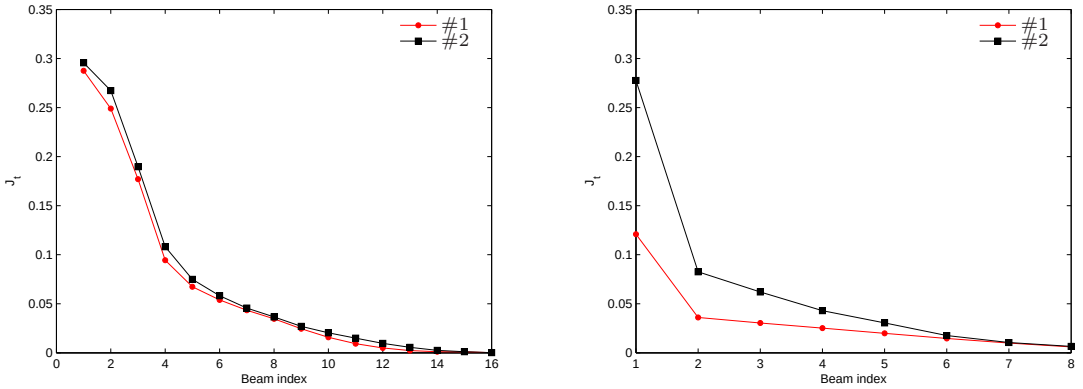

(a) Wing (b) Vertical tail

Figure 21. Updated torsional constants with constraint on aerodynamic derivatives.

been presented together with an overview of the methods adopted for linear static aeroelasticity. Future works will also enhance the optimization process with flutter constraint in terms of minimum damping allowed.

Acknowledgments

The financial support by the European Commission through co-funding of the FP6 project SimSAC is acknowledged.

References

[1]Raymer, D. P., *Aircraft Design: A Conceptual Approach, Fourth Edition*, AIAA Education Series, New York, NY, 2006.

[2]Torenbeek, E., *Synthesis of Subsonic Airplane Design*, Kluwer Academic Pub, Delft University Press, 1982.

[3]Lucia, D. J., "The SensorCraft Configurations: A Non-Linear AeroServoElastic Challenge for Aviation," *Proceedings of the 46th AIAA/ASME/ASCE/AHS/ASC SDM Conference*, Austin, Texas, 18 - 21 April 2005.

[4]Silva, W. A., Vartio, E., Shimko, A., Kvaternik, R. G. and, E. K. W., and Scott, R., "Development of Aeroservoelastic Analytical Models and Gust Load Alleviation Control Laws of a SensorCraft Wind-Tunnel Model Using Measured Data," *Proceedings of the IFASD International Forum on Aeroelasticity*, Stockholm, June 17 - 20 2007.

[5]Liebeck, R. H., "Design of the BlendedWing Body Subsonic Transport," *Journal of Aircraft*, Vol. 41, No. 1, January-February 2004, pp. 10–25.

[6]Antoine, N., Kroo, I., Willcox, K., and Barter, G., "A Framework for Aircraft Conceptual Design and Environmental Performance Studies," *Proceedings of the 10th AIAA/ISSMO Multidisciplinary Analysis and Optimization Conference*, Albany, New York, 30 August - 1 September 2004 2004.

[7]Kroo, I. and Shevell, R., "Aircraft Design: Synthesis and Analysis," Tech. rep., http://adg.stanford.edu/aa241/AircraftDesign.html, September 2006.

[8]Ning, S. A. and Kroo, I., "Tip Extensions, Winglets, and C-wings: Optimization in Conceptual Wing Design," Tech. rep., http: //aero.stanford.edu/adgreports.html, August 2008.

[9]Macci, S. H., "Semi-analytical method for predicting wing structural mass," Tech. rep., SAWE Paper No.2282, May 1995.

[10]Bindolino, G., Ghiringhelli, G., and Ricci, S., "Preliminary Sizing Of The Wing-Box Structure By Multi-Level Approach," *Int. Forum on Aeroelasticity and Structural Dynamics IFASD 2005, - Munich, Germany*, June 28 - July 01 2005.

[11]Isikveren, A., *Quasi-analytical modelling and optimization techniques for transport aircraft design*, Ph.D. thesis, Royal Institute of Technology (KTH), 2002.

[12]SimSAC, "`http://www.simsacdesign.eu/`," last accessed 2009.

[13]Von Kaenel, R., Rizzi, A., Grabowski, T., Ghoreyshi, M., Cavagna, L., Ricci, S., and Bérard, A., "Bringing Adaptive-Fidelity CFD to Aircraft Conceptual Design: CEASIOM." *Proceedings of the* 26th *ICAS Congress*, Anchorage, Alaska, 14–19 September 2008.

[14]Bérard, A., Rizzi, A., and Isikveren, A., "CADac: A New Geometry Construction Tool for Aerospace Vehicle Pre-Design and Conceptual Design," *Proceedings of the* 26th *AIAA Applied Aerodynamics Conference*, Honolulu, Hawaii, 18–21 August 2008.

[15]Mitchell, C., "A Computer Programme to Predict the Stability and Control Characteristics of Subsonic Air-

craft," Report TR 73079, Royal Aircraft Establishment, Procurement Executive, Ministry of Defence, September 1973.

[16]Perez, R. E., Jansen, P. W., and Martins, J. R. R. A., "Aero-Structural Optimization of non-planar lifting surface configurations," *Proceedings of the* 12th *AIAA-ISSMO Multidisciplinary Analysis and Optimization Conference*, Victoria, British Columbia, 10–12 September 2008.

[17]Ardema, M., Chambers, A., Hahn, A., Miura, H., and Moore, M., "Analytical Fuselage and Wing Weight Estimation of Transport Aircraft," Tech. Rep. 110392, NASA, Ames Research Center, Moffett Field, California, May 1996.

[18]Mason, W. H., "`http://www.aoe.vt.edu/~mason/Mason_f/MRsoft.html/`," LDSTAB software, last accessed 2009.

[19]Shanley, F. R., *Weight-strength analysis of aircraft structures*, Dover Publications, Inc., New York, 2nd ed., 1960.

[20]Niu, M. C., *Airframe Structural Design*, Hong Kong Conmilit Press Ltd, Honk Kong, 1st ed., 1988.

[21]Gerard, G., "Optimum Structural Design Concepts for Aerospace Vehicles," *Journal of Spacecraft and Rockets*, Vol. 3, No. 1, January 1966, pp. 5–18.

[22]Crawford, R. F. and Burns, A. B., "Minimum weight potentials for stiffened plates and shells," *AIAA Journal*, Vol. 1, No. 4, 1963, pp. 879–886.

[23]Moran, J., *An Introduction to Theoretical and Computational Aerodynamics*, John Wiley & Sons, 1984.

[24]Katz, J. and Plotkin, A., *Low-Speed Aerodynamics From Wing Theory to Panel Methods*, McGraw-Hill series in Aeronautical and Aerospace Engineering, 1991.

[25]Albano, E. and Rodden, W. P., "A Doublet–Lattice Method for Calculating the Lift Distributions on Oscillating Surfaces in Subsonic Flow," *AIAA Journal*, Vol. 7, No. 2, 1969, pp. 279–285.

[26]Chen, P. C. and Liu, D. D., "A Harmonic Gradient Method for Unsteady Supersonic Flow Calculations," *Journal of Aircraft*, Vol. 22, No. 15, 1985, pp. 371–379.

[27]Cavagna, L., Quaranta, G., and Mantegazza, P., "Application of Navier-Stokes simulations for aeroelastic assessment in transonic regime," *Computers & Structures*, Vol. 85, No. 11-14, 2007, pp. 818–832, Fourth MIT Conference on Computational Fluid and Solid Mechanics.

[28]Ghiringhelli, G. L., Masarati, P., and Mantegazza, P., "A Multi-Body Implementation of Finite Volume Beams," *AIAA Journal*, Vol. 38, No. 1, January 2000, pp. 131–138.

[29]Masarati, P. and Mantegazza, P., "On the C^0 Discretisation of Beams by Finite Elements and Finite Volumes," *l'Aerotecnica Missili e Spazio*, Vol. 75, 1997, pp. 77–86.

[30]Kier, T. M., "Comparison of Unsteady Aerodynamic Modelling Methodologies with respect to Flight Loads Analysis," *Proceedings of the AIAA Atmospheric Flight Mechanics Conference and Exhibit*, San Francisco, California, 15–18 August 2005.

[31]Smith, M. J., Hodges, D. H., and Cesnik, C. E., "Evaluation of Computational Algorithms for Suitable Fluid-Structure Interactions," *Journal of Aircraft*, Vol. 37, No. 2, 2000, pp. 282–294.

[32]Bathe, K.-J. and Zhang, H., "Finite Element Developements for General Fluid Flows with Structural Interactions," *International Journal for Numerical methods in Engineering*, Vol. 60, 2004, pp. 213–232.

[33]Quaranta, G., Masarati, P., and Mantegazza, P., "A Conservative Mesh-free Approach for Fluid-Structure Interface Problems," *International Conference on Computational Methods for Coupled Problems in Science and Engineering*, edited by M. Papadrakakis, E. Oñate, and B. Schrefler, CIMNE, Santorini, Greece, 2005.

[34]Beckert, A. and Wendland, H., "Multivariate Interpolation for Fluid-Structure-Interaction Problems Using Radial Basis Functions," *Aerospace Science and Technology*, Vol. 5, 2001, pp. 125–134.

[35]Schaback, R. and Wendland, H., "Characterization and Construction of Radial Basis Functions," *EILAT Proceedings*, edited by N. Dyn, D. Leviatan, and D. Levin, Cambridge University Press, 2000.

[36]Canavin, J. R. and Likins, P. W., "Floating reference frames for flexible spacecraft," *Journal of Spacecraft*, Vol. 14, No. 12, December 1977, pp. 724–732.

[37]Haftka, R. T. and Gürdal, Z., *Elements of structural optimization*, Dordrecht, 3rd ed., 1992.

[38]Österheld, C. M., Heinze, W., and Horst, P., "Influence of Aeroelastic Effects on Preliminary Aircraft Design," *Proceedings of the* 22th *ICAS Congress*, Harrogate, UK, 27 August – 1 September 2000.